https://doi.org/10.5194/acp-2020-213
Preprint. Discussion started: 18 May 2020

Atmospheric Chemistry and Physics Discussions

Seasonal variations in the high time-resolved aerosol composition, sources, and chemical process of background submicron particles in North China Plain

Jiayun Li[1, 4], Liming Cao[2], Wenkang Gao[1], Lingyan He[2]; Yingchao Yan[1,4], Dongsheng Ji[1], Zirui Liu[1], Yuesi Wang[1,3,4]

[1]State Key Laboratory of Atmospheric Boundary Layer Physics and Atmospheric Chemistry (LAPC), Institute of Atmospheric Physics, Chinese Academy of Sciences, Beijing 100029, China
[2]Key Laboratory for Urban Habitat Environmental Science and Technology, Peking University Shenzhen Graduate School, Shenzhen, 518055, China
[3]Center for Excellence in Regional Atmospheric Environment, Institute of Urban Environment, Chinese Academy of Sciences, Xiamen 361021, China
[4]University of Chinese Academy of Sciences, Beijing 100049, China

Correspondence: Zirui Liu (liuzirui@mail.iap.ac.cn); Lingyan He (hely@pkusz.edu.cn)
Jiayun Li and Liming Cao contributed equally to this work.

Abstract. For the first time in the North China Plain (NCP), we investigated the seasonal variations of submicron particles ($NR\text{-}PM_1$) and its chemical composition at a background mountain station using Aerodyne high-resolution time-of-flight aerosol mass spectrometry (HR-ToF-AMS). The averaged $NR\text{-}PM_1$ were highest in autumn (15.1μg m^{-3}) and lowest in summer (12.4 μg m^{-3}), with the abundance of more nitrate in spring (34%), winter (31%), and autumn (34%), and elevated organics (40%) and sulfate (38%) proportion in summer. The submicron particles were almost neutralized by excess ammonium in all four seasons except summer, when the aerosol particles appeared to be slightly acidic. The size distribution of all PM_1 species showed a consistent accumulation mode peaked at approximately 600-800 nm (dva), indicating the highly aged and internally mixed nature of the background aerosols, which further supported by the source appointment using multilinear engine (ME-2) and significant contributions of aged secondary organic aerosol (SOA) in organic aerosol (OA) were resolved in all seasons (>77%), especially in summer (95%). The oxidation degree and evolution process of OAs in the four seasons were further investigated, and enhanced carbon oxidation state (-0.45-0.10), O/C (0.54-0.75) and OM/OC (1.86-2.13) ratios compared with urban studies were observed, with the highest oxidation degree of which appeared in summer, likely due to the relatively stronger photochemical processing which dominated the processes of both less oxidized OA (LO-OOA) and more oxidized OA (MO-OOA) formations. Aqueous-phase processing also contributed to the SOA formation but prevailed in autumn and winter and the role of which to MO-OOA and LO-OOA also varied in different seasons. In addition, compared with the urban atmosphere, LO-OOA formation in the background atmosphere exhibited more regional characteristics, as photochemical and aqueous-phase processing enhanced during the transport in summer and autumn, respectively. Furthermore, the backward trajectories analysis showed that higher submicron particles were associated with air mass for short distance transported from the southern regions in four seasons, while the long-range transport from Inner Mongolia (west and north regions) also contributed to the summer particle pollutions in the background areas of NCP. Our results illustrate the background particles in NCP are influenced significantly by aging processing and transport, and the more neutralized state of submicron particles

https://doi.org/10.5194/acp-2020-213
Preprint. Discussion started: 18 May 2020

Atmospheric Chemistry and Physics Discussions

with the abundance of nitrate compared with those in the background atmosphere in southern and western China, highlighting the regional reductions in emissions of nitrogen oxide and ammonia are critical for remedying the increased occurrence of nitrate-dominated haze event in the NCP.

1. Introduction

With rapid industrialization, population expansion and urbanization, the North China Plain (NCP) has been seriously polluted in recent years (Tao et al., 2012;Du et al., 2015;Yuan et al., 2015;Zhao et al., 2019). The formation mechanisms of particulate pollution are complex because of the unfavorable meteorological conditions, complex source emissions, and geographical conditions. For example, sulfate dominated the secondary inorganic aerosols in industrialized cities located in the south of the NCP, while in recent years, nitrate dominated the secondary inorganic aerosols in the north of the NCP (Huang et al., 2018;Li et al., 2019a). High relative humidity (RH) favored heterogeneous reactions and hygroscopic growth, leading to an increase in secondary aerosols and further aggravating haze pollution in the NCP (Sun et al., 2013a;Liu et al., 2016). Moreover, haze pollution in the NCP can be exacerbated by its unique topography. Hu et al. (2014) found that heat from the Loess Plateau could be transported to the plain with westerly airflow, resulting in enhanced thermal inversion and suppressing the planetary boundary layer (PBL), thus weakening atmospheric diffusion. Furthermore, the southern NCP is an important pathway for water vapor and pollutant transport in the PBL because of the blocking effect of the Taihang Mountains (Tao et al., 2012).

Nearly all previous researches on the characterizations of fine particles in the NCP were conducted on heavily polluted urban or suburban stations with strong local source emissions, while a few studies have been deployed at the background station. Early studies at the background site in the NCP were mainly focused on the average chemical compositions, source analysis, and the influence of regional transportation (Pan et al., 2013;Liu et al., 2018), which indicated that secondary aerosols dominated the aerosol particles at background sites and that regional transport affected the air pollution the background atmosphere. However, these studies at the background site in the NCP were limited by the low resolution of one or several days.

The high-resolution time-of-flight aerosol mass spectrometry (HR-ToF-AMS) has been widely used to characterize nonrefractory submicron particles (NR-PM_1) at numerous urban sites and a few background sites on the Qinghai–Tibet Plateau (QTP) in western China, the Lake Hongze site in northern China and the Mount Wuzhi site in southern China (Zhang et al., 2019b;Xu et al., 2018;Du et al., 2015;Zhu et al., 2016). The high-resolution characterization of PM_1 species in the background atmosphere in the NCP is limited. Until recently, Li et al. (2019b) deployed combined measurements of submicron aerosols at an urban and a background station in the NCP using a HR-ToF-AMS and a quadrupole AMS, respectively. The results showed that nitrate accounted for the highest proportions of PM_1 in winter, which was affected by local chemical production and

https://doi.org/10.5194/acp-2020-213
Preprint. Discussion started: 18 May 2020


Atmospheric Chemistry and Physics Discussions

regional transportation, OA was also highly oxidized during regional transport. However, since the meteorological conditions and emission sources changed from season to season, these findings may not be applicable in other seasons. Few observations of PM_1 chemical components in the regional background area in the NCP using HR-TOF-AMS covering four seasons have been reported. Moreover, a previous study in Xinglong (Li et al., 2019b) was based on unit mass resolution, without elemental information and only one secondary organic aerosol (OOA) factor identified in the study. The HR-ToF-AMS can provide elemental information, such as hydrogen-to-carbon (H/C), organic-mass-to-organic-carbon (OM/OC), and oxygen-to-carbon (O/C), which can help to quantify the oxidation degree of OA (Jimenez, 2003). OOA can also be separated as more-oxidized OOA (MO-OOA) and less-oxidized OOA (LO-OOA) due to the different O/C ratios (Zhang et al., 2011). The formation and evolution of LO-OOA and MO-OOA vary greatly in different areas and seasons, mainly due to the complex interaction of local emissions, chemical reactions, and meteorological influences. For example, photochemical processing dominated the oxidized degree of OA in haze events, whereas aqueous-phase processing was the main reason that affected the oxidized degree of OA in foggy events in Hong Kong (Li et al., 2013;Qin et al., 2016). In urban Beijing, Xu et al. (2017) found that aqueous-phase processing dominated MO-OOA formation in all seasons. While in Li's et al (2020) study, the impact of photochemistry on MO-OOA formation enhanced as the photochemical age increased in early autumn in Beijing. Therefore, the evolution and formation mechanisms of the OOA productions in the NCP are still unclear, especially in the background atmosphere because of the higher atmospheric oxidation capacity and oxidation degree of OA in the background areas than in urban areas. Deeply exploring the characterization of the seasonal variations in PM_1 and the formation and evolution of the two OOA productions in the background atmosphere during different seasons based on field observations using HR-ToF-AMS is of great significance.

In this study, a HR-ToF-AMS with instruments for the measurement of meteorological parameters and gaseous parameters was first deployed during four seasons at the Xinglong background station to investigate the seasonal variations in PM_1 species in the background atmosphere in the NCP. The seasonal variations in the submicron aerosols, including the variation in the mass concentrations, chemical composition, aerosol acidity, size distribution, diurnal variation, and meteorological effects, were presented in detail in this study. The seasonal sources, oxidization degrees, and evolution processes of OOA productions were fully explored. Finally, back trajectory analyses were performed to investigate the different pathways and the regional transport influences of the background atmospheric aerosols during the four seasons in the NCP.

2. Experimental methods

2.1 Sampling sites

The Xinglong background station is located in the north of Hebei Province, south of Yanshan Mountains, 960 meters above sea level, with longitude and latitude of 117.67° and 40.40°, respectively, about 115 kilometers northeast of Beijing (Pan et al., 2013). Since Xinglong station is surrounded by forests and there are no serious pollutant emissions in this area, it

https://doi.org/10.5194/acp-2020-213
Preprint. Discussion started: 18 May 2020


Atmospheric Chemistry and Physics Discussions

can be considered as an ideal station to investigate haze episodes in the NCP on a regional scale. More details about Xinglong station can be found everywhere (Li et al., 2019b;Tian et al., 2018).

2.2 Instrumentation and operation

From March to December 2019, a HR-ToF-AMS was deployed to measure the mass concentrations and chemical compositions of NR-PM_1. The sampling periods were from May 1 to 31, June 20 to July 26, October 12 to November 12, and November 25 to December 25 in 2019. The ambient particles were sampled into the AMS through a URG cyclone (URG-2000-30ED) for removing coarse particles with size cutoffs of 2.5 μm, which was followed a Nafion dryer to dry the sampled aerosols to eliminate the impact of high humidity on particles. During these four campaigns, both of the "V" and "W" modes were operated and the time resolution was 3 min. The HR-ToF-AMS calibrations were carried out in strict according to the standards reported in previous studies (Jimenez, 2003;Zhang et al., 2014a).

Simultaneously, other measurements also deployed during the whole campaign. Specifically, a Sharp-5030 was used to measure the total PM_1 concentration. Gaseous species including Ozone (O_3), nitric oxide (NO), nitrogen dioxide (NO_2), carbon monoxide (CO), and sulfur dioxide (SO_2) were measured by the Thermo gas analyzers. Milos520 (Vaisala, Finland) was used to obtain the meteorological parameters. More details about the instruments can be seen in Li et al. (2019b).

2.3 Data analysis

The analysis softwires of SQUIRREL (v1.57H) and PIKA (v1.16H) were used to analyze the size-resolved mass concentrations and the mass spectra of OA, respectively. According to Canagaratna et al. (2015), the improved-ambient method was used to obtain the elemental compositions ratios. The particle collection efficiency (CE) was applied to account for the incomplete detection of particles due to particle bounce (Aiken et al., 2009). According to Middlebrook et al. (2012), the CE value can be affected by the RH, aerosol acidity, and the ammonium nitrate mass fractions (ANMF). The ambient aerosols were dried by a Nafion dryer. Meanwhile, Aerosols were neutral in spring, autumn, and winter, and weakly acidic in summer (Fig. 2). Therefore, RH and aerosol acidity could not influence the CE values in all seasons. However, the ANMF values were normally above 0.4 in spring, autumn, and winter, indicating that NH_4NO_3 would substantially affect the CE values in these three seasons. Combined with the analysis of the above three aspects, a constant CE of 0.5 was used in summer, and the CE values in the other three seasons were calculated according to Middlebrook et al. (2012)(CE = max (0.45, 0.0833+0.9167*ANMF)).

The PMF Evaluation Tool PET (v3.04A; (Ulbrich et al., 2009)) were first performed for the OA source apportionment in each season. The error matrix was modified, ions with low signal to noise ratios were down-weighted or removed. It was common to use PMF analyses to identify the sources of OA. However, it was difficult to distinguish similar factors in areas with complex pollution sources. Due to the high fraction of OOA in OA, it is of great difficulty to separate POA from OOA in

https://doi.org/10.5194/acp-2020-213
Preprint. Discussion started: 18 May 2020


Atmospheric Chemistry and Physics Discussions

Xinglong using the PMF analysis, because the POA factor is easily mixed with the OOA factor. For example, for spring, according to the PMF analysis (Fig. S2), in the two- to four-factor solutions, POA factors were mixed with OOA factors because the HOA profile contains a higher-than-expected contribution from m/z 44. In the 5-factor solution, a POA factor appeared, while OOA was oversplit, some of which showed similar characteristics. The POA was finally identified as fossil fuel OA (FFOA), which is a typical profile in Xinglong. Details about the diagnosis information can be seen in Sect. 3.2. Therefore, the multilinear engine (ME-2) was also used, which constrained the prior known source information. Specifically, we constrained the FFOA profile separated by the five-factor solution of PMF analysis in spring during all seasons to better separate FFOA from OOA. The a value of 0-0.5 with a space of 0.1 in each season was used to constrain the FFOA profiles to explore the solution space (Canonaco et al., 2013). As a result, three OA factors, including FFOA, LO-OOA, and MO-OOA, were identified with ME-2 analysis in each season (Fig. S2-S3).

2.4. Backward trajectory modeling

The 48 h back trajectories were calculated every hour at a height of 500 m using the HYSPLIT-4.8 (Hybrid Single-Particle Lagrangian Integrated Trajectories) model in each season in this study. Meteorological data was archived from the Air Resource Laboratory, NOAA, and the resolution was 1° × 1°. The cluster analysis algorithm was used to classify the back trajectories of each season.

3 Results and discussion

3.1 Mass concentrations of PM_1 species

3.1.1 Seasonality of the chemical composition of PM_1

The annual mean mass concentrations of organic, nitrate, sulfate, ammonium, and chlorine in PM_1 were 4.6, 4.8, 2.8, 2.2, and 0.1 μg m^{-3}, respectively, totaling 14.5 μg m^{-3}. This total PM_1 concentration was much lower than the values observed in urban and suburban areas in the NCP, such as 81 μg m^{-3} in urban Beijing (Hu et al., 2017), 187 μg m^{-3} in urban Handan and 178 μg m^{-3} in urban Shijiazhuang in Hebei Province in winter (Li et al., 2017;Huang et al., 2018), and 52 μg m^{-3} at suburban Gucheng station (Zhang, 2011). It was higher than those in national background areas in eastern and western China, such as 9.1 μg m^{-3} at the Waliguan background station in summer, 4.4 μg m^{-3} at the south edge of the QTP in spring, and 10.9 μg m^{-3} at the Mount Wuzhi station in spring (Zhang et al., 2019b;Zhu et al., 2016). The higher PM_1 mass concentration in Xinglong in the background atmosphere in the NCP compared to those in other remote areas in eastern and western China indicated the air pollution in the NCP is serious.

Seasonally, the average PM_1 concentrations were 13.7, 12.4, 15.1, and 14.1 μg m^{-3} in the four seasons, respectively. OA showed the highest portion in NR-PM_1 in summer, accounting for 40% by mass. Nitrate was the highest secondary inorganic

https://doi.org/10.5194/acp-2020-213
Preprint. Discussion started: 18 May 2020

Atmospheric Chemistry and Physics Discussions

aerosol (SIA) components in spring (34%), winter (31%), and autumn (34%). The low percentage of nitrate in summer (9.6%) could be attributed to the higher temperature than in other seasons, which suppresses the partitioning to particulate nitrate (Seinfeld and Pandis, 2016). Sulfate remained relatively low in spring (16%), autumn (21%), and winter (19%), but it increased to 38% of the NR-PM_1 mass in summer. Ammonium accounted for 13-17% of PM_1 concentrations in all four seasons.

As shown in Fig.1, the proportions of OA in PM_1 gradually decreased as PM_1 increased in all seasons, suggesting that the enhanced SIA dominated the increase in PM_1, similar to the findings of previously reported researches (Hu et al., 2017;Zhang et al., 2019b). The proportions of nitrate in PM_1 slightly increased in spring, summer, and autumn, corresponding to the increase in RH, suggesting that aqueous-phase reactions could be conducive to nitrate production. It was worth noting that the RH in spring was generally lower than those in autumn and winter. For example, when the PM_1 concentrations were higher than 40 μg m^{-3}, the RH was above 40% in autumn and winter, but below 40% in spring. This might be attributed to the frequent dust events in spring, which was often accompanied by the dry and cold air from the northern regions. As a result, aqueous-phase reactions might be more conducive to nitrate formation in autumn and winter than in spring. In winter, the decreased percentage of nitrate with a high PM_1 concentration (PM_1 > 50 μg m^{-3}) was due to the increase in sulfate because of the coal emissions during the heating season. The proportions of ammonium remained stable in all seasons even when the PM_1 concentration was low, suggesting that ammonia is excessive in the NCP. Although the average PM_1 concentrations in the four seasons were similar (Table1), the frequency distribution of PM_1 showed strong seasonal dependency. High frequency and extremely low frequency of PM_1 concentrations were observed when the PM_1 concentration was below 10 μg m^{-3} and above 40 μg m^{-3}, respectively, in spring, autumn, and winter. In summer, the frequency distribution of PM_1 did not change dramatically as PM_1 increased.

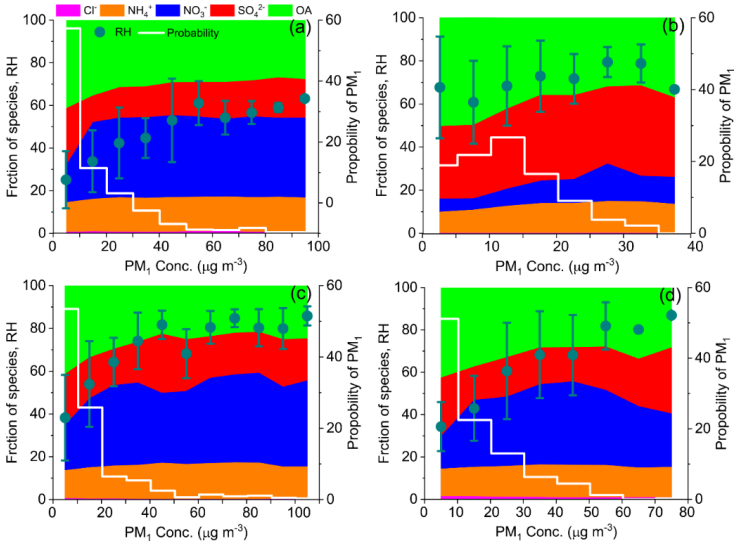

Figure 1. Fractions of PM_1 species in PM_1 as a function of PM_1 concentrations and the probability density of PM_1 (white curves) in (a) spring, (b) summer, (c) autumn, and (d) winter. The average values and standard deviations of RH are illustrated.

https://doi.org/10.5194/acp-2020-213
Preprint. Discussion started: 18 May 2020

Atmospheric Chemistry and Physics Discussions

3.1.2 Seasonality of aerosol acidity

The acidity of PM_1 in the four seasons was also evaluated. Particles are deemed to be mostly neutralized when $[NH_4^+]_{meas}/[NH_4^+]_{neu} \approx 1$ according to Zhang et al. (2007). The submicron aerosols in Xinglong were almost completely neutralized by the excess ammonium in spring, autumn, and winter, especially in spring and autumn, which was supported by the scatter plot between the measured and predicted ammonium concentrations in Fig. 2 (slope=0.93 in spring; slope=0.89 in autumn; slope=0.85 in winter). The relatively neutral atmosphere in spring could be attributed to the large amount of mineral dust. A previous study showed that the mineral dust in Xinglong accounts for about 10% of the aerosols in summer, autumn, and winter and as much as 34% in spring (Huang et al., 2017). The aerosols in winter were slightly more acidic than those in autumn because of the increased percentage of sulfate, which was related to coal combustion during the heating period.

The almost neutral aerosol in Xinglong in these three seasons was consistent with the value observed in Beijing (Li et al., 2018) in the NCP but different from the results obtained at lightly polluted urban sites and background sites in southern and western China where the aerosol particles were generally weakly acidic due to the high fraction of sulfate (Zhang et al., 2019b;Xu et al., 2018), suggesting more rigorous measures should be implemented to reduce NOx and ammonia emissions in northern China. This conclusion could be further demonstrated by previous studies showing that the effective control of emissions from coal combustion in the NCP results in the increase of ammonia and decrease of sulfur dioxide in the atmosphere, which is beneficial to form ammonium nitrate (NH_4NO_3) (Zhang et al., 2019a;Wang et al., 2019). In summer, the aerosol particles appeared to be slightly acidic because of the decreased proportion of nitrate and increased proportion of sulfate to PM_1, which could be mainly attributed to the evaporative loss of NH_4NO_3. Aerosol particles in Xinglong were almost neutralized by excess ammonium in all four seasons except summer, which indicated that the emission of nitrogen oxide and ammonia should be reduced on a regional scale in the NCP.

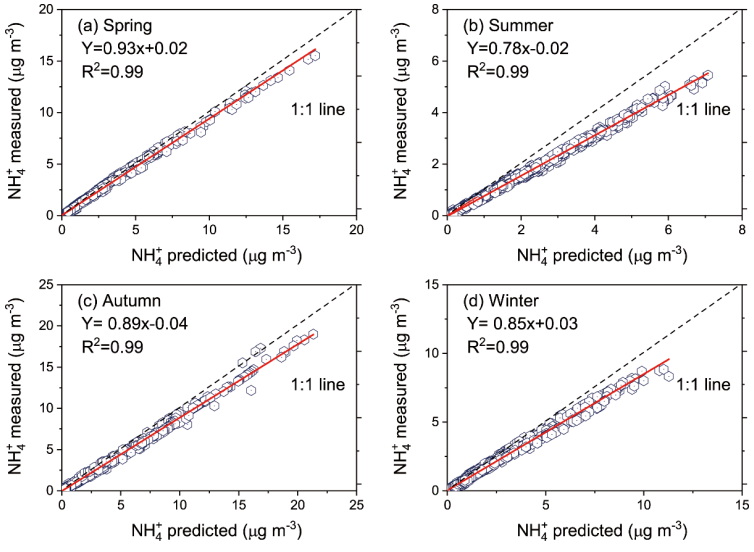

Figure 2. Scatter plot and linear regression of measured NH_4^+ and predicted NH_4^+ in (a) spring, (b) summer, (c) autumn, and

https://doi.org/10.5194/acp-2020-213
Preprint. Discussion started: 18 May 2020

Atmospheric Chemistry and Physics Discussions

(d) winter.

3.1.3 Seasonality of meteorological effects on PM_1 species

The chemical composition of PM_1 exhibited distinctive characteristics in the four seasons, which was due to the significant seasonal variation in meteorological conditions and emissions. As shown in Table 1, the NOx showed higher concentration in winter, suggesting the stronger influence of traffic-related emissions from heavily polluted regions to Xinglong in winter than in other seasons. SO_2 concentrations were low in all seasons and showed no obvious seasonal changes (1.0-1.9 ppb). O_3 concentration was highest in summer, likely due to the high temperature and enhanced photochemical processing.

Table 1. Seasonal variations in average meteorological parameters, gaseous precursors, and NR-PM_1 species. The data here are listed in the form of "average ± standard deviation".

	Spring	Summer	Autumn	Winter
	1 May-31 May	22 Jun-27 Jul	11 Oct-11 Nov	25 Nov-26 Dec
Meteorological parameters				
T (℃)	3.9 ± 4.7	21.4 ± 3.9	8.1 ± 3.9	-5.1 ± 3.1
RH (%)	31 ± 17	68 ± 19	49 ± 23	44 ± 20
WS (m s^{-1})	3.3 ± 1.3	2.0 ± 1.3	2.1 ± 1.3	2.4 ± 1.4
P (Hpa)	913 ± 4	906 ± 3	918 ± 5	920 ± 5
Gaseous precursors				
O_3 (ppb)	48 ± 11	78 ± 24	37 ± 13	29 ± 8
NO (ppb)	0.2 ± 0.2	0.2 ± 0.3	0.4 ± 0.8	0.7 ± 1.4
NO_2 (ppb)	4.0 ± 4.0	4.0 ± 2.0	12 ± 7	14 ± 10
NOx (ppb)	4.3 ± 4.1	4.3 ± 2.2	13 ± 9	15 ± 11
SO_2 (ppb)	1.0 ± 1.2	1.9 ± 1.7	1.3 ± 1.7	0.7 ± 1.2
CO (ppm)	0.55 ± 0.41	0.49 ± 0.25	0.54 ± 0.22	0.59 ± 0.33
Aerosol species /μg m^{-3}				
Org	4.5 ± 4.7	11.5 ± 10.6	5.0 ± 4.5	4.8 ± 3.8
FFOA	0.7 ± 0.7	4.9± 2.6	0.7 ± 0.5	1.1 ± 0.9
LO-OOA	1.2 ± 1.7	1.6 ± 1.2	1.7 ± 2.2	1.2 ± 1.2
MO-OOA	2.8 ± 2.8	3.2 ± 1.8	2.6 ± 2.1	2.3 ± 2.0
SO_4^{2-}	2.2 ± 2.6	4.6 ± 3.1	3.1 ± 4.0	2.7 ± 2.8
NO_3^-	4.7 ± 6.3	1.2 ± 14	5.1 ± 7.6	4.4 ± 5.2

https://doi.org/10.5194/acp-2020-213
Preprint. Discussion started: 18 May 2020

Atmospheric Chemistry and Physics Discussions

NH_4^+	2.1 ± 2.6	1.6 ± 1.2	2.3 ± 3.0	2.0 ± 2.0
Cl^-	0.1 ± 0.1	0.01 ± 0.02	0.04 ± 0.06	0.2 ± 0.2
NR-PM_1	13.7 ± 16.0	12.4 ± 7.4	15.1 ± 18.7	14.1 ± 13.3

Horizontal wind speed could affect the diffusion and transportation of pollutants. In spring and winter, with the increase of the wind speed, the concentrations of almost all PM_1 species decreased, suggesting the impact of dilution of winds on atmospheric aerosols (Fig. 3). However, the wind dilution ratios were much lower than the observed value in urban Beijing in winter (Li et al., 2019b), but comparable to the value observed at a rural station (Wang et al., 2016), suggesting that aerosols in the background atmosphere were homogeneously distributed. Therefore, the winds showed a weaker influence in terms of diluting aerosol particles than the result observed in Beijing. In autumn, PM_1 species only decreased rapidly when WS > 4 m/s, while secondary inorganic aerosols increased rapidly from 1 to 4 m s^{-1}, suggesting the significant role of an intermediate wind speed in secondary inorganic aerosol transport, similar to the findings of a previous study conducted in autumn in Xinglong (Li et al., 2019b). In summer, all PM_1 species decreased gradually as the wind speed increased, except OA and sulfate, suggesting the strong influence of regional transport on OA and sulfate formation, especially OA formation. The relationship between pollutants and wind direction in summer also differed from that in other seasons. All PM_1 species showed high concentrations in association with wind from the southern regions and low concentrations in association with wind from the northern regions in spring, autumn, and winter. In summer, PM_1 species also showed relatively high concentrations in association with wind from the northeast regions. Results here might indicate the effect of the regional transport from southern heavily polluted regions on atmospheric aerosols at the regional background site in the NCP in all seasons and that northern transport might also partially contributes in summer.

As shown in Fig. 3, we also investigated the effects of RH on the secondary aerosols. When RH < 80%, secondary inorganic aerosols (SIA) (especially nitrate) increased significantly as RH increased in autumn and winter, suggesting the significant effect of aqueous-phase reactions on SIA formation. Previous studies in urban Beijing showed a successive increase in SIA with the increase of RH (Li et al., 2019b;Liu et al., 2016), which suggested that the aqueous-phase processing affected nitrate formation in both urban and background atmospheres. The WS also increased rapidly as RH increased from 60% to 80% and then maintained a high level in autumn in Xinglong, while WS continually decreased as RH increased at urban sites in the NCP (Huang et al., 2018;Li et al., 2019b). This behavior further indicates regional transport has more influence on the SIA concentration in the background atmosphere than in the urban atmosphere in the NCP in autumn. In spring, SIA only increased significantly at moderate RH levels as RH increased (<60%), suggesting a weaker impact of aqueous-phase processing on SIA formation in spring than in autumn and winter. When RH > 60%, the SIA concentrations decreased rapidly, and this decrease was accompanied by a rapid decrease in wind speed, suggesting the impact of regional transport also weakened. Notably, the OA and sulfate concentrations were high even when RH was low (RH < 40) in summer, which was significantly different from

https://doi.org/10.5194/acp-2020-213
Preprint. Discussion started: 18 May 2020

Atmospheric Chemistry and Physics Discussions

what occurred in other seasons, suggesting the impact of photochemistry on the formation of sulfate and OOA. Furthermore, OA did not increase as RH increased in summer, which suggested the different formation mechanisms of OA in summer than in other seasons, which was specifically investigated in Sect. 3.4.

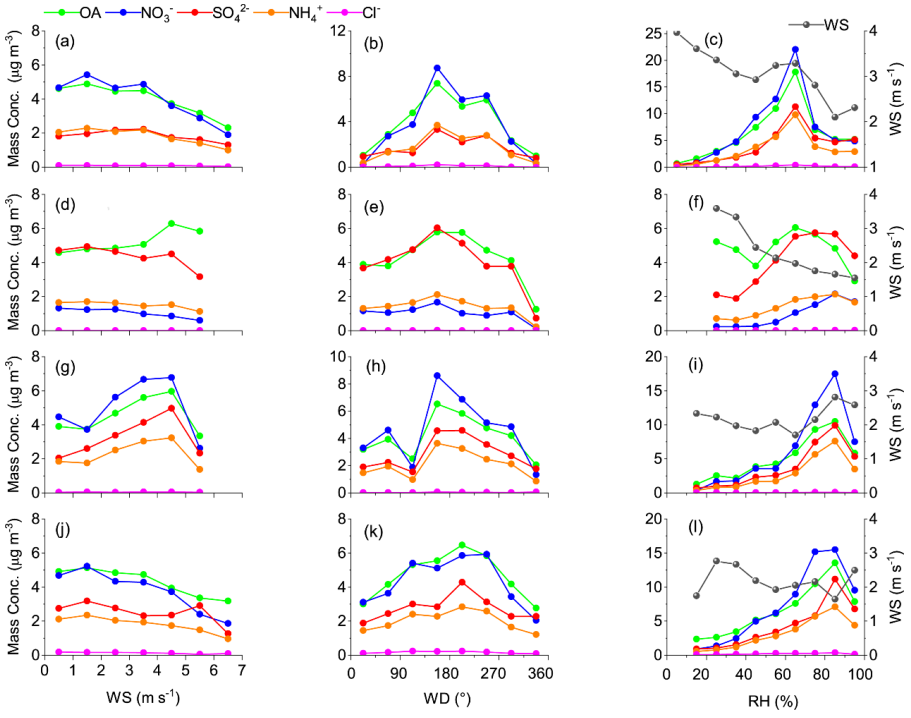

Figure 3. Variations in mass concentrations of PM_1 species as functions of WS, WD, and RH in (a) spring, (b) summer, (c) autumn, and (d) winter. (OA: organic aerosol).

3.1.4 Seasonality of the size distribution of the chemical components of PM_1

The size distribution of all PM_1 species in each season concentrated in accumulation mode (Fig. 4), with a peak diameter at approximately 600-800 nm (dva), indicating aerosols in the background atmosphere were highly aged and internally mixed (Jimenez, 2003). Compared to Beijing, OA in Xinglong had a larger peak diameter and a wider size distribution in each season (Hu et al., 2017). Compared to SIA, OA always had a higher concentration in small size (100-500 nm) mode in urban areas, likely caused by the existence of strong primary OA (POA) emissions (Zhang et al., 2014a;Liu et al., 2016). However, in Xinglong, the peak diameters of OA were close to those of SIA in the four seasons, indicating OA was highly oxidized in Xinglong.

The size distributions of SIA showed similar shapes in spring and autumn and peaked at approximately 700 nm, suggesting internally mixed (Liu et al., 2016). The mode diameters of the SIA in Xinglong (700-750 nm) were higher than those in Beijing (600–650 nm) in spring and summer (Hu et al., 2017). The differences in SIA peak diameters may be caused by the stronger photochemical activity and long-range transport in Xinglong than in Beijing in these two seasons. The peak

https://doi.org/10.5194/acp-2020-213
Preprint. Discussion started: 18 May 2020

Atmospheric Chemistry and Physics Discussions

diameter of sulfate in summer was the highest in four seasons, indicating that the sulfate was highly aged in summer in the NCP. The peak diameters (550-700 nm) of PM_1 species in winter were lower than those in the other three seasons, which might be attributed to the relatively higher existence of the primary emissions in winter. What's more, the greater new particle formation in winter also resulted in smaller average sizes (Hu et al., 2016).

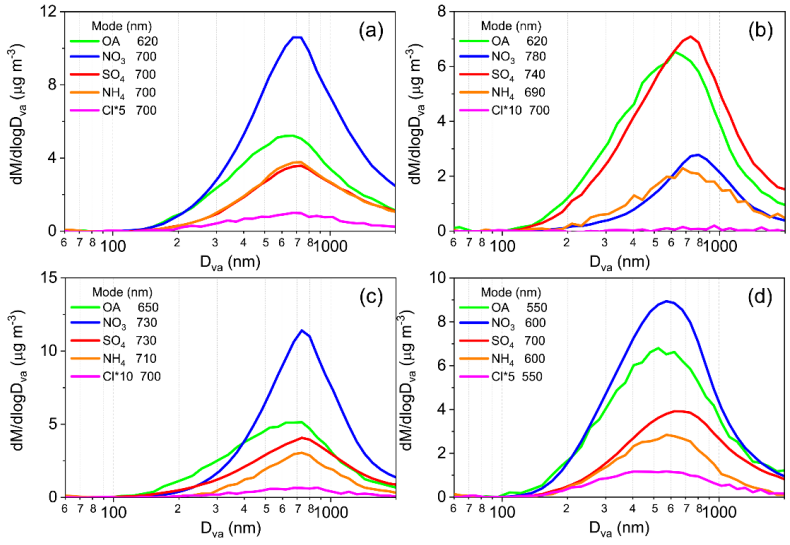

Figure 4. Mass size distributions of PM_1 species in (a) spring, (b) summer, (c) autumn, and (d) winter.

3.2 OA source appointment

Due to the high fraction of OOA in OA, it is of great difficulty to separate POA from OOA in Xinglong using the PMF analysis, because the POA factor is easily mixed with the OOA factor. For example, for spring, according to the PMF analysis (Fig. S2), in the two- to four-factor solutions, POA factors were mixed with OOA factors because the HOA profile contains a higher-than-expected contribution from m/z 44. In the 5-factor solution, a POA factor appeared, while OOA was oversplit, some of which showed similar characteristics.

The mass spectrum (MS) pattern of the POA factor (factor3) mainly consisted of hydrocarbon ions ($C_nH_{2n+1}^+$ and $C_nH_{2n-1}^+$), which are commonly related to combustion emissions (Zhang et al., 2015;Sun et al., 2013b). The POA factor correlated well with NOx, indicating that the POA factor was closely related to the traffic-related emissions (Hu et al., 2017). These characteristics suggested that the POA factor was similar to hydrocarbon-like OA (HOA). But unlike the mass spectrum of HOA, coal combustion-related ions (e.g., m/z 77, 91, and 115) also accounted for approximately 1% of the POA factor. The high correlation coefficient between the POA factor and chloride further proved the significant contribution of coal combustion to the POA factor in Xinglong. What's more, HOA and coal combustion OA (CCOA) show the remarkably similar MS pattern when m/z was below 120 (Sun et al., 2016;Sun et al., 2018), which is sometimes difficult to be separated by PMF analysis, so

https://doi.org/10.5194/acp-2020-213
Preprint. Discussion started: 18 May 2020


Atmospheric Chemistry and Physics Discussions

that FFOA can be considered as a combined factor of HOA and CCOA (Sun et al., 2018). In this study, it was difficult to separate CCOA form HOA because of the low percentage of POA in OA. Therefore, the POA factor in this study could also be considered as FFOA, which is a typical profile in Xinglong.

We constrained the FFOA profiles separated by the five-factor solution of PMF analysis in spring during all seasons to better separate FFOA from OOA. As a result, three OA factors, including FFOA, LO-OOA, and MO-OOA, were identified with ME-2 analysis in each season (Fig. S2-S3). The O/C ratios of the FFOA factors were 0.15, 0.12, 0.15, and 0.11 during the four seasons, respectively. The proportions of FFOA to OA were relatively low in all seasons (5-23%), especially in summer (5%), mainly due to the low anthropogenic emissions around Xinglong station. The concentrations of FFOA were higher at night than during the daytime during the four seasons, indicating relatively high primary emissions at night.

The high f44 values were permanent in the MS of both LO-OOA and MO-OOA. The f44 values for MO-OOA and LO-OOA in the four seasons ranged from 16.3 to 23.5%, 8.1 to 13.8%, respectively. The f43 values for MO-OOA and LO-OOA ranged from 4.8 to 5.2%, 6.8 to 9.1%, respectively. These behaviors indicated that MO-OOA had a higher oxidation degree than LO-OOA. The O/C ratios of the MO-OOA factors in the four seasons were 0.93, 0.94, 0.84, and 0.80, respectively, higher than those in the corresponding LO-OOA (0.69, 0.63, 0.67, and 0.57). In addition, MO-OOA and LO-OOA correlated well with sulfate and nitrate, respectively, which may further suggest the different origination of these two oxygenated OA.

OOA accounted for as much as 77-95% of the OA in the four seasons (Fig. 5). The percentages of OOA in OA during all seasons in Xinglong were much higher than those in urban Beijing (48-68%; (Hu et al., 2017)), slightly higher than the results observed at national background stations in Waliguan (75%; (Zhang et al., 2019b)) in western China and in Lake Hongze in northern China (70%; (Zhu et al., 2016)), and comparable with those observed in a less-polluted atmosphere in Hong Kong (80-85%; (Li et al., 2015)) and a rural site in Xingzhou in central China (82%; (Wang et al., 2016)) but lower than that observed at a national background station in Mount Wuzhi in eastern China (100%; (Zhu et al., 2016)). These characteristics indicate the occurrence of highly oxidized OA in Xinglong, which may be attributed to the high oxidizing ability and the strong impact of regional transportation in the background atmosphere in the NCP.

https://doi.org/10.5194/acp-2020-213
Preprint. Discussion started: 18 May 2020

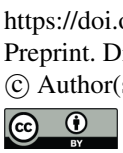

Atmospheric Chemistry and Physics Discussions

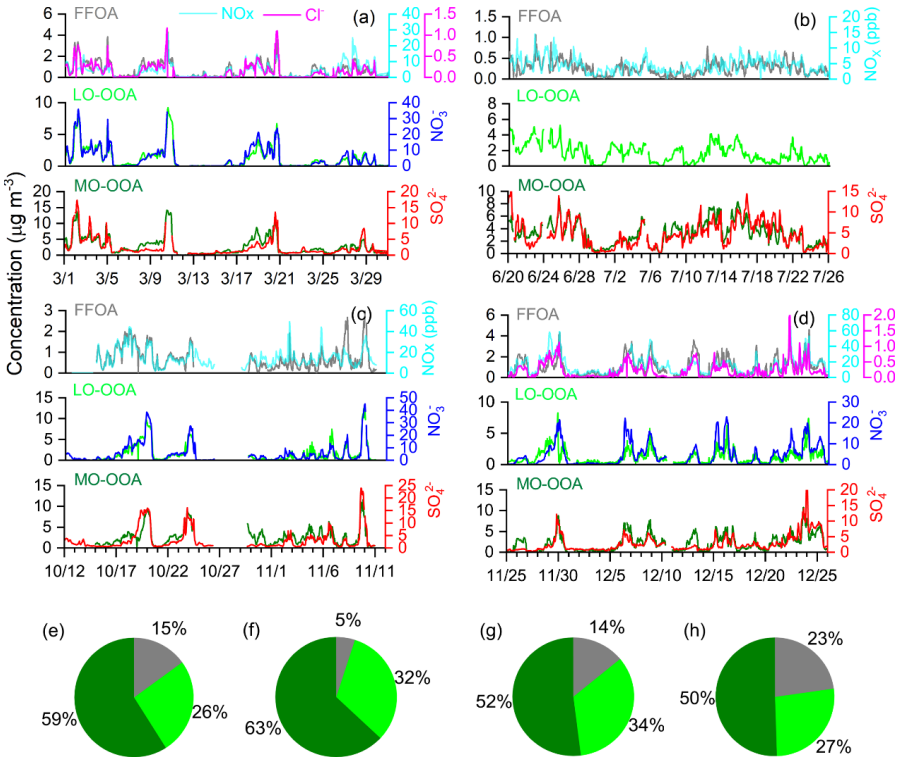

295

Figure 5. Time series of three OA factors in (a) spring, (b) summer, (c) autumn, and (d) winter: FFOA, LO-OOA, and MO-OOA. The time series of NOx, chloride, nitrate, and sulfate are shown for comparison. The pie charts depict the average OA compositions in (e) spring, (f) summer, (g) autumn, and (h) winter.

3.3 Diurnal variations

300 As shown in Fig. 6, nitrate concentration was higher at night than during the daytime in each season, suggesting the strong pathway of the hydrolysis of N_2O_5 to nitrate formation at night in Xinglong due to low NO concentration and the high O_3 concentration even at night. The NO concentrations in Xinglong Station in the four seasons were as low as 0.2 to 0.7 ppb (Table 1). Because of the low concentration of NO, it is difficult for NO to react with O_3 and thus deplete O_3 so that O_3 can be accumulated even at night. O_3 concentrations as night in the four seasons were about 45, 70, 35, 25 ppb, respectively, which
305 showed that the background atmosphere exhibited high atmospheric oxidation capacity even at night, especially in summer. Nitrate exhibited the lowest concentration in summer, which can be attributed to the evaporation of NH_4NO_3 due to the high temperatures (Fig. 6). Interestingly, the nitrate concentration increased rapidly from noon to the afternoon in spring, autumn, and winter, which may imply the significant role of regional transport in these three seasons, whereas the contribution of regional transport to nitrate in summer would be weakened because of the evaporation of NH_4NO_3. These characteristics of
310 the nitrate diurnal pattern indicate the strong effects of local chemical production and regional transport on nitrate formation

https://doi.org/10.5194/acp-2020-213
Preprint. Discussion started: 18 May 2020


Atmospheric Chemistry and Physics Discussions

in the background atmosphere.

In comparison to the diurnal patterns of nitrate, sulfate showed flatter diurnal cycles in each season, showing the regional characteristics. In summer, sulfate increased rapidly from noon to evening, and the wind speed and O_3 concentration increased significantly, indicating the strong influence of the regional transport of sulfate and O_3 in summer. Specifically, the wind speed in autumn and winter increased slightly from 8:00 to 14:00 from about 1.8 to 2.8 m s^{-1}. However, in summer, the wind speed increased rapidly from 8:00 to 16:00 from 0.7 to 2.8 m s^{-1} and the O_3 concentration increased significantly from 60 to 88 ppb, with an increase rate of 3.5 ppb h^{-1} at the same time. As a result, photochemical processing enhanced sulfate formation during the regional transport during the daytime. At night, however, the high sulfate concentration might be attributed to the enhancement of aqueous-phase processing under high temperatures and humidity (Zhang et al., 2014b).

The MO-OOA showed similar diurnal cycles in the four seasons, increasing from noon to evening, with the results showing the regional characteristics of MO-OOA formation. These characteristics were similar to the results found in previous researches conducted in urban Beijing showing that LO-OOA is mainly formed by local chemical reactions, but MO-OOA formation exhibits regional characteristics. However, in Xinglong, LO-OOA formation also showed regional characteristics in summer and autumn, as LO-OOA slightly increased from noon to evening. This behavior suggests that LO-OOA in the background atmosphere might be more aged than those in the urban atmosphere in the NCP. In summer, both LO-OOA and MO-OOA showed daytime increases, corresponding to the increase in O_3 at the same time, suggesting the strong impact of photochemistry on LO-OOA and MO-OOA in Xinglong.

The primary components, chlorine, and FFOA, exhibited similar diurnal variations, with the lowest concentrations in summer and the highest concentrations in winter. What's more, both chlorine and FFOA showed flat diurnal cycles in summer, but dramatic diurnal cycles in winter with high concentrations at night and low concentrations during the daytime. These characteristics could be attributed to the relatively high emissions in winter and the suppressed boundary layer at night.

https://doi.org/10.5194/acp-2020-213
Preprint. Discussion started: 18 May 2020

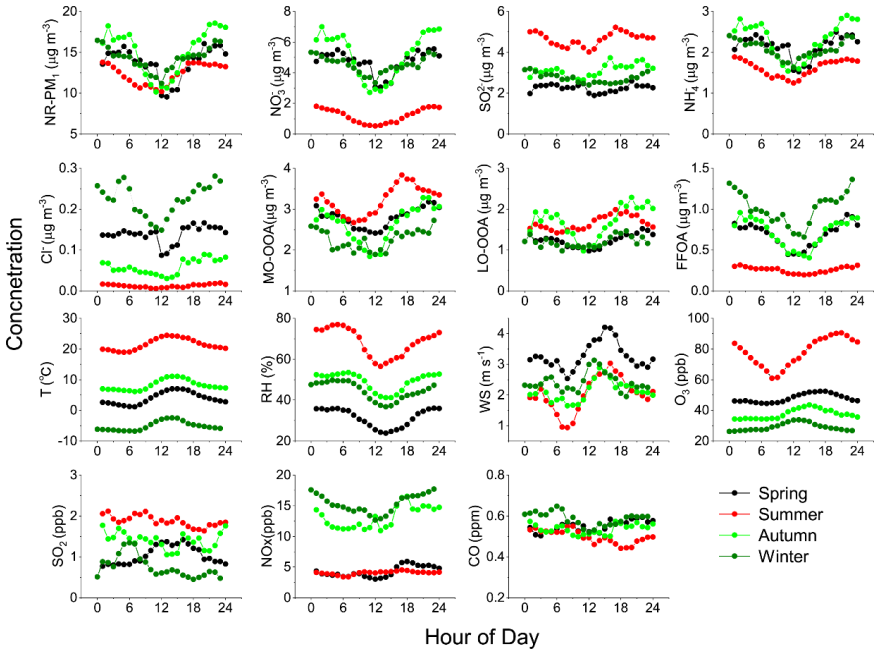

Figure 6. Diurnal variations in meteorological parameters, gaseous precursors, and PM_1 species in four seasons.

3.4 SOA chemistry and oxidation state

3.4.1 Oxidation state of OA and SOA

As shown in Table 2, during the four seasons in this study, the average O/C and H/C ratios, OM/OC ratios, and carbon oxidation state (OSc) were in the range of 0.54-0.75, 1.41-1.53, 1.86-2.13, and -0.45-0.10, respectively. The O/C ratio was highest in summer (0.75), second highest in spring (0.71), and lowest in winter (0.54). The high O/C ratios in summer (0.75) were also observed in urban Beijing and suburban areas of Hong Kong, indicating strong OOA formation via photochemical processing in summer. The low O/C ratios in winter (0.54) were related to a higher proportion of POA in OA than in other seasons. The O/C ratios in Xinglong in all seasons (0.54-0.75) were slightly higher than those in urban Beijing (0.47-0.53), mainly due to the strong presence of primary organic emissions, such as traffic-related and cooking-related emissions. Meanwhile, the O/C ratios in Xinglong in all seasons were much higher than those obtained at rural/suburban sites in China and in western countries, e.g., Hong Kong (0.38-0.52), Kaiping (0.47), Fresno (0.35), Melpitz (0.52-0.54) and Mexico City (0.53) (Li et al., 2015;Huang et al., 2011;Poulain et al., 2011;Aiken et al., 2009;Ge et al., 2012;Hu et al., 2017), suggesting the organic aerosols in Xinglong were highly aged. In addition, the O/C ratios in Xinglong in the four seasons were comparable with that observed at the background Lake Hongze site in northern China. The slightly higher O/C ratios of OA in national background areas in eastern and western China, such as 0.99 at the Waliguan background station in summer and 0.98 at the Mount Wuzhi site in spring (Zhang et al., 2019b;Zhu et al., 2016) was due to the highly aged air mass during the long-range

https://doi.org/10.5194/acp-2020-213
Preprint. Discussion started: 18 May 2020


Atmospheric Chemistry and Physics Discussions

transport. Overall, the oxidized degree of OA in Xinglong was far higher than those at urban/rural/suburban sites and comparable with those at background sites in eastern and western China.

Table 2. Elemental ratios and OSc in OA obtained from field observations at the background, rural/suburban, and urban sites.

Site	Site types	Periods	O/C	H/C	OM/OC	Osc	References
Xinglong (China)	Background	Spring	0.71	1.44	2.08	-0.01	This study
		Summer	0.75	1.41	2.13	0.10	
		Autumn	0.61	1.47	1.94	-0.26	
		Winter	0.54	1.53	1.86	-0.45	
Lake Hongze (China)		Spring	0.67	1.52		-0.18	(Zhu et al., 2016)
Mount Wuzhi (China)		Spring	0.98	1.32		0.64	(Zhu et al., 2016)
Waliguan (China)		Summer	0.99	1.43	2.44	0.55	(Zhang et al., 2019)
Hongkong (China)	Rural/Suburban	Spring	0.38	1.35	1.64	-0.59	(Li et al., 2015)
		Summer	0.52	1.36	1.84	-0.32	
		Autumn	0.42	1.39	1.71	-0.55	
		Winter	0.43	1.4	1.71	-0.54	
Kaiping (China)		Autumn	0.47	1.48	1.77	-0.54	(Huang et al., 2011)
Melpitz (Germany)		Summer	0.52	1.51	1.83	-0.47	(Poulain et al 2011)
		Autumn	0.54	1.48	1.84	-0.4	
		Winter	0.53	1.48	1.83	-0.41	
Beijing (China)	Urban	Spring	0.49	1.63	1.81	-0.64	(Hu et al., 2017)
		Summer	0.53	1.61	1.88	-0.54	
		Autumn	0.46	1.58	1.77	-0.66	
		Winter	0.47	1.52	1.79	-0.58	
Mexico City (Mexico)		Spring	0.53	1.82	1.73	-0.77	(Aiken et al., 2009)
Fresno, CA (US)		Winter	0.35	1.75	1.63	-1.05	(Ge et al., 2012)

Figure 7 shows the comparison of the O/C ratios of OOA, LO-OOA, and MO-OOA in a variety of environments grouped into two types according to their location: urban and suburban/rural/background sites. For some sites, only one OOA factor was identified, while for others, two OOA factors, including LO-OOA and MO-OOA factors, were identified according to the different oxidation states. For the later sites, the average O/C ratios of OOA can be reconstructed as a mass-weighted average of the O/C ratios of LO-OOA and MO-OOA according to Ng et al. (2010). The O/C ratios of OOA in Xinglong in the four

https://doi.org/10.5194/acp-2020-213
Preprint. Discussion started: 18 May 2020

Atmospheric Chemistry and Physics Discussions

seasons (0.8-0.93) were comparable with that observed at background Lake Hongze site (0.89) in northern China, lower than those observed in national background areas in eastern and western China, which was due to the highly aged air mass during the long-range transport in national background areas. These results highlighted the high atmospheric oxidizing capacity in background areas in both southern and northern China. The O/C ratios of OOA in Xinglong was far higher than those ratios obtained at urban sites in lightly polluted areas, e.g., Hong Kong and Fresno, and those in suburban/rural/downwind areas, e.g., Jiaxing, Kaiping and Hong Kong, and comparable to those in urban Beijing in the NCP in the four seasons (Li et al., 2015;Huang et al., 2011;Ge et al., 2012;Huang et al., 2013;Hu et al., 2017;Xu et al., 2014). The comparable O/C ratios of the OOA in Xinglong and Beijing (Hu et al., 2017) in winter were probably due to the relatively higher proportion of POA in the OA than in the other seasons. Although the O/C ratios of OOA in Xinglong and Beijing were comparable and both at high levels, the formation mechanisms of OOA were distinct at the two sites, and a detailed discussion is provided in Sect. 3.4.2.

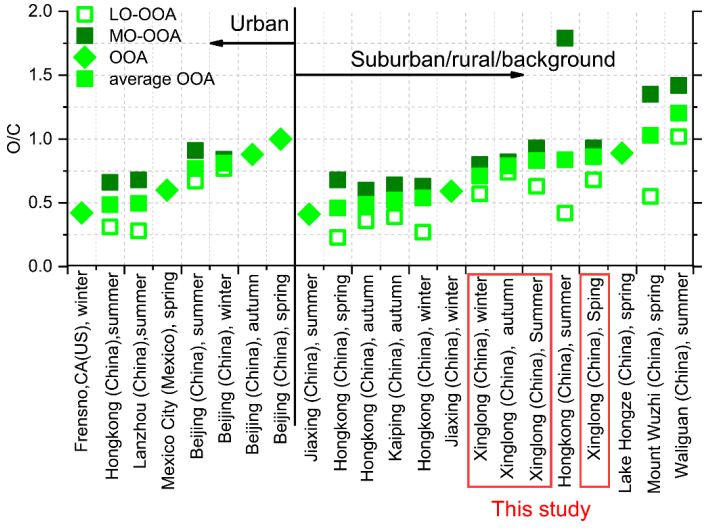

Figure 7. Estimated O/C ratios of OOA, LO-OOA, and MO-OOA at each site. The mass-weighted average OOA component is also shown for sites in which LO-OOA and MO-OOA are both resolved. (Note: MO-OOA and LO-OOA are identified as LV-OOA and SV-OOA, respectively)

3.4.2 Evolution and formation of SOA

As shown in Fig. 8, the effects of aqueous-phase processing on the formation of LO-OOA and MO-OOA differed in the four seasons. Both LO-OOA and MO-OOA increased significantly as RH increased when RH < ~90% in autumn and winter and then decreased. This behavior suggested aqueous-phase processing had a significant influence on OOA formation in these two seasons. In spring, LO-OOA and MO-OOA only increased under moderate RH (RH< 70%) as RH increased. Notably, Ox did not increase as RH increased in autumn and winter but increased when RH < 70% as RH increased in spring. These behaviors suggest that aqueous-phase processing affects OOA production in autumn and winter more than in spring and that

https://doi.org/10.5194/acp-2020-213
Preprint. Discussion started: 18 May 2020

Atmospheric Chemistry and Physics Discussions

380 photochemical processing may partially contribute to OOA production in spring. According to Xu et al., (2017), aqueous-phase processing promotes MO-OOA formation but suppresses LO-OOA formation in urban Beijing, suggesting a more significant role of aqueous-phase processing in LO-OOA production in the background atmosphere than in the urban atmosphere in autumn and winter. The increases of LO-OOA and MO-OOA under moderate RH condition in spring (50%<RH<70%) were associated with the slight increase of wind speed, and the rapid decrease of which when RH > 70% also 385 corresponded to the rapid decrease in wind speed (Fig. 8(i)) and Ox, suggesting the decreased transport of OA and photochemical ability under high RH conditions, which suppressed OOA production. While in autumn, the increases of LO-OOA and MO-OOA under high RH condition (70%<RH<90%) were associated with the significant increase of average wind speed from 1.8 to 2.9 m s^{-1} (Fig. 8(k)), which facilitated the transport of water vapor and pollutants from the heavily polluted southern regions. Results here indicated the important role of regional transport in LO-OOA and MO-OOA formation in 390 autumn, as aqueous-phase processing enhanced during the transport.

In summer, MO-OOA increased as RH (40% < RH < 60%) increased. However, LO-OOA showed a continuously decreasing trend as RH increased in summer, except for a slightly increasing trend when RH increased from 40 to 60%, suggesting a weak influence of aqueous-phase processing on LO-OOA formation. Results here illuminate that the moderate RH conditions (50%<RH<70%) in summer promote the formation of MO-OOA but suppress that of LO-OOA. Moreover, the 395 concentrations of the two OOA productions were high with low RH (RH < 40%) which was distinct from the pattern observed in other seasons, indicating the more significant influence of photochemical processing on OOA formation in summer. This was further confirmed by the high Ox concentration (~85 ppb) when RH < 40%. Different variations in the O/C ratios of OA were observed in the four seasons. Clear increases in the O/C ratios of OA as RH increased were observed in all seasons except summer, suggesting the impact of aqueous-phase processing on the oxidation degree of OA in spring, autumn, and winter.

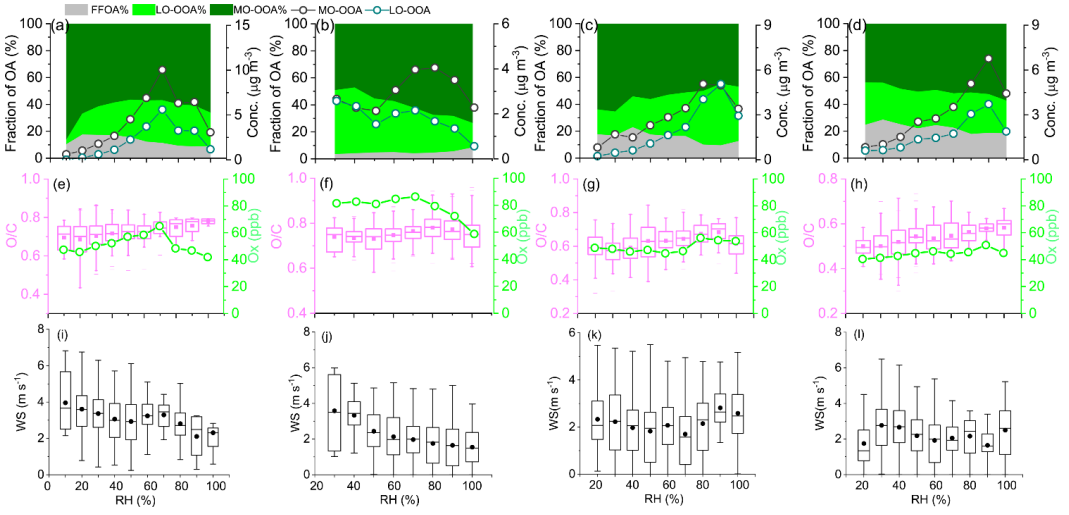

400

Figure 8. Variations in the mass concentrations of FFOA, LO-OOA and MO-OOA and the fractions of OA factors in OA,

https://doi.org/10.5194/acp-2020-213
Preprint. Discussion started: 18 May 2020

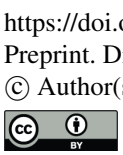

Atmospheric Chemistry and Physics Discussions

O/C, Ox, and WS as a function of RH in (a, e, i) spring, (b, f, j) summer, (c, g, k) autumn, and (d, h, l) winter. The data were binned according to the RH (10% increment).

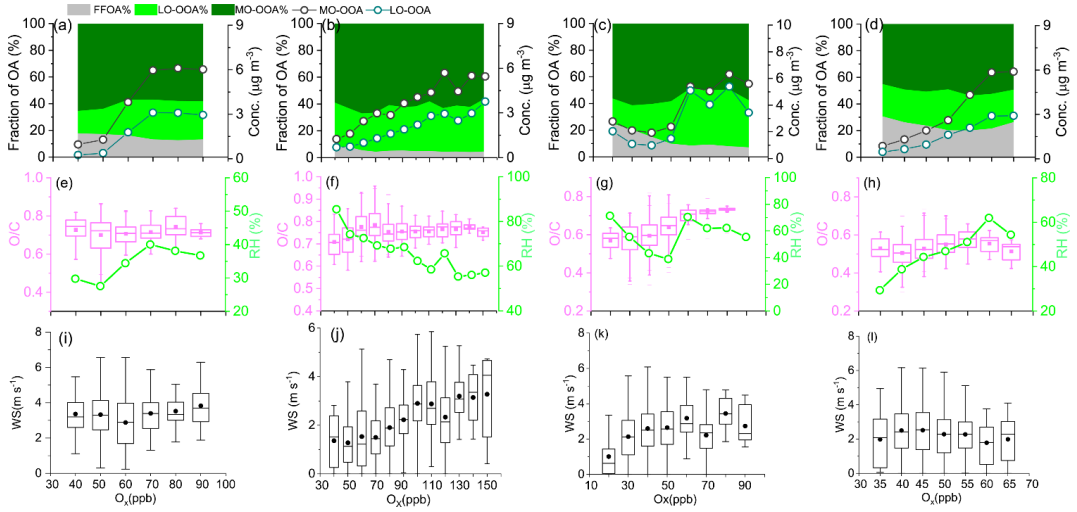

405 **Figure 9.** Variations in the mass concentrations of FFOA, LO-OOA and MO-OOA and the fractions of OA factors in OA, RH, and WS as a function of RH in (a, e, i) spring, (b, f, j) summer, (c, g, k) autumn, and (d, h, l) winter. The data were binned according to the Ox (10ppb increment in spring, summer, and autumn; 5ppb increment in winter).

As shown in Fig. 9, the effects of photochemistry on the formation of LO-OOA and MO-OOA were also investigated. LO-OOA and MO-OOA increased rapidly at moderate Ox levels when Ox changed from 50 to 70 ppb, 40 to 60 ppb, and 45 410 to 60 ppb in spring, autumn, and winter, respectively, and then remained unchanged at high Ox levels, suggesting that photochemical processing also contributes to LO-OOA and MO-OOA production in these three seasons. Notably, RH also showed a significant increase and high levels (~ 60%) when Ox changed from 50 to 60 ppb in autumn and from 45 to 60 ppb in winter. This behavior further indicates that aqueous-phase processing plays a more important role than photochemical processing in OOA production in autumn and winter. In spring, RH maintained low levels (RH < 40%) as Ox increased, further 415 confirming the weaker impact of aqueous-phase processing on OOA production in spring than in autumn and winter. In summer, both LO-OOA and MO-OOA showed overall increasing trends as Ox increased, while RH showed a corresponding overall decreasing trend. Furthermore, the average wind speed increased as Ox increased, which was more significant than those in other seasons. These characteristics indicate the stronger influence of photochemical processing on both LO-OOA and MO-OOA production than that of aqueous-phase processing. What's more, photochemical processing enhanced during regional 420 transport in summer. In urban Beijing, the impact of photochemical processing on LO-OOA production was significant, while on MO-OOA production was limited in summer (Xu et al., 2017), mainly due to the higher atmospheric oxidation capability in the background atmosphere than in the urban atmosphere in summer.

https://doi.org/10.5194/acp-2020-213
Preprint. Discussion started: 18 May 2020


Atmospheric Chemistry and Physics Discussions

3.5 Transport pathways

To explore the transport pathways and the effects of regional and long-distance transport on fine particles at the background site in the NCP, we calculated the backward trajectories of PM_1 species with TrajStat and the HYSPLIT-4.8 model in four seasons. Both (Fig. 10) long-distance transport and regional air masses influenced Xinglong. Based on the distances over which the air masses were transported, the clusters during the four seasons were defined as short, medium, and long transport pathways. Specifically, clusters 1 in spring, 4 in summer and autumn, and 3 in winter were defined as short transport pathways. Clusters 1, 2, and 3 in summer, cluster 2 in autumn, and cluster 2 in winter were considered medium transport pathways. Clusters 2 and 3 in spring, cluster 5 in summer, clusters 1 and 3 in autumn, and cluster 1 in winter were considered long transport pathways.

The short-distance trajectories originated in the southwest/southeast of Xinglong, areas that suffer from serious pollution. The southwest trajectories started in south Hebei Province and passed over Beijing. The southeast trajectories started at the Bohai Sea and extended through Tianjin and Tangshan. Although the three short-distance clusters account for only 15-44% of all the air masses during each season, the PM_1 concentrations for the short-distance clusters from the southern regions were the highest of all the clusters, indicating that aerosol particles at Xinglong station were greatly affected by the regional transport from southern regions.

The long-distance trajectories mainly from the further northwest regions of Xinglong and northeast regions also partially contribute in summer. The long-distance clusters account for 16-56% of all the clusters in spring, autumn, and winter, while they only account for 4% in summer. The long-distance clusters bring less-polluted aerosols from the northern regions. These results were also supported by the low PM_1 concentrations of 3.3-4.9 μg m^{-3} associated with the long-distance trajectories. Relatively smaller peak diameters were also found for the chemical components related to the long-distance clusters, suggesting that the aerosols were relatively fresh, while the larger peak diameters for the short-distance clusters indicated that the aerosols were more aged (Fig. S4).

During the seasonal observations in Xinglong, the pathways of the dominant air masses differed. The medium-distance clusters (clusters 1, 2, and 3) were dominant in summer and are representative of a regional-scale transport path. The transport distances of the air masses from southern regions (Cluster 1) were longer than those in other seasons (cluster 1 in spring, cluster 4 in autumn, and cluster 3 in winter), suggesting the stronger influence of southern regional transport to Xinglong in summer. Cluster 1 in summer started at Bohai Bay and passed through the Shandong Peninsula and over Bohai Bay. The PM_1 concentrations for clusters 1 (14.3 μg m^{-3}) and 4 (13.9 μg m^{-3}) were both high. Additionally, the air masses from the southern regions (clusters 1 and 4) account for 70% of all the air masses in summer, which was obviously higher than the percentages in other seasons (15-44%), further confirming the dominant role of southern transport in submicron aerosols in the NCP in summer. Furthermore, the transport distances of clusters from the north and west regions in summer were shorter than those

https://doi.org/10.5194/acp-2020-213
Preprint. Discussion started: 18 May 2020

Atmospheric Chemistry and Physics Discussions

in other seasons. In general, with the decrease in the transport distance of clusters from the north and west regions, particle concentration gradually increased (Hu et al., 2017). The peak diameters of OA with air masses from the west and north regions in summer (~680 nm) were obviously higher than those in other seasons (450-600 nm), suggesting more aged aerosols in association with clusters from the west and north regions in summer (Fig. S4). Although the clusters from these regions in summer only accounted for 13% and 12% of all the air masses, respectively, the PM_1 concentrations for the two clusters (cluster 3: 10.1 μg m^{-3}; cluster 2: 11.5 μg m^{-3}) were both at high levels and similar to those associated with the south air masses (cluster 4: 13.9 μg m^{-3} and cluster 1: 14.3 μg m^{-3}). All these characteristics suggest that regional transport from Inner Mongolia (west and north regions of Xinglong) also partially contributes to the particle pollution in the background area of the NCP in summer.

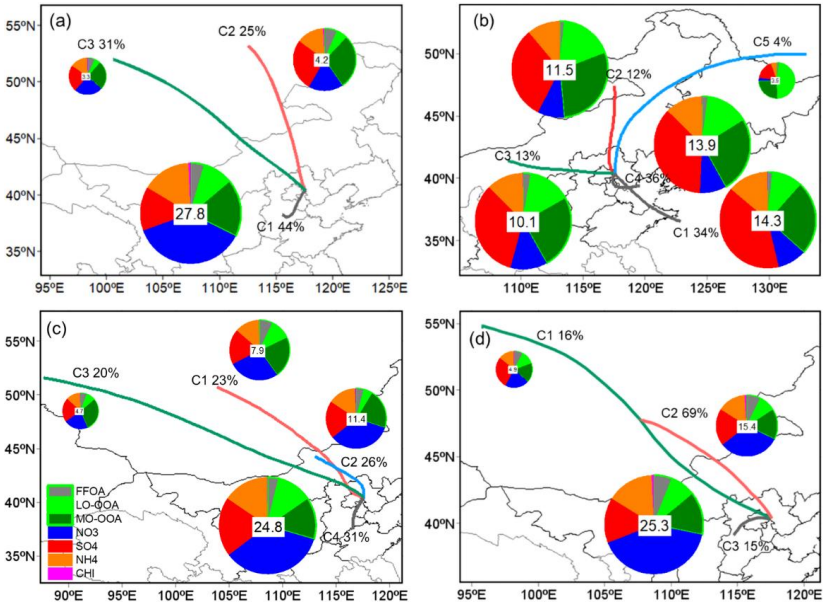

Figure 10. The average 48 h backward air mass trajectories clusters calculated at 1 h intervals in spring (a), summer (b), autumn (c), and winter (d). The percentages of PM_1 species in PM_1 in each air mass trajectories clusters were shown in the pie charts with the average PM_1 concentrations marked in the center of the pie charts.

4. Conclusion

The chemical components in PM_1 were investigated during four seasons at a background station in the NCP using a HR-ToF-AMS measurement. The average mass concentrations of NR-PM_1 in the four seasons of spring, summer, autumn, and winter were 13.7, 12.4, 15.1, and 14.1 μg m^{-3}, respectively. OA contributed the most to PM_1 in summer, accounting for 40% by mass. Nitrate was the greatest SIA component in spring (34%), winter (31%), and autumn (34%), while sulfate was the highest SIA component in summer (38%). Considering the aerosol particles were almost neutralized by excess ammonium in

https://doi.org/10.5194/acp-2020-213
Preprint. Discussion started: 18 May 2020


Atmospheric Chemistry and Physics Discussions

all four seasons except summer, the emission of nitrogen oxide and ammonia should be reduced on a regional scale. The size distribution of all PM_1 species showed a consistent accumulation mode peaked at approximately 600-800 nm (dva), indicating the highly aged and internally mixed nature of the background aerosols.

ME-2 analysis was used to analyze the HRMS in Xinglong in the four seasons and identified three OA factors, including FFOA, LO-OOA, and MO-OOA. SOA (LO-OOA+MO-OOA) dominated OA as much as 77-95% in the four seasons, especially in summer (95%). The oxidation degree and evolution process of OAs in the four seasons were further investigated, and enhanced carbon oxidation state (-0.45-0.10), O/C (0.54-0.75) and OM/OC (1.86-2.13) ratios compared with urban studies were observed, with the highest oxidation degree of which appeared in summer, likely due to the relatively stronger photochemical processing which dominated the processes of both LO-OOA and MO-OOA formations. Aqueous-phase processing also contributed to the SOA formation but prevailed in autumn and winter and the role of which to MO-OOA and LO-OOA also varied in different seasons. In addition, LO-OOA formation in the background atmosphere exhibited more regional characteristics in autumn and winter than those in the urban atmosphere, where LO-OOA was mainly formed by local chemical reactions. Regional transport also contributed significantly to LO-OOA formation in the background atmosphere, as photochemical and aqueous-phase processing enhanced during the transport in summer and autumn, respectively.

The backward trajectories analysis showed that higher PM_1 concentrations were from the southern regions of Xinglong with shorter transport distances in spring, autumn, and spring, while in summer, regional transport from Inner Mongolia (west and north regions of Xinglong) also partially contributed to the pollution in the NCP because of the similar PM_1 concentrations with air masses from Inner Mongolia and southern regions of Xinglong. Moreover, the influence of regional transport from the southern regions of Xinglong to the NCP was strongest in summer because of the longer transport distance of air masses from the southern regions in summer than in other seasons.

Our results illustrate the background particles in NCP are influenced significantly by aging processing and regional transportation, which was similar with those background aerosols in southern and western China. Whereas, submicron particles at the background areas of NCP are more neutralized with the abundance of nitrate, compared with those in the background atmosphere in southern and western China, highlighting the regional reductions in emissions of nitrogen oxide and ammonia are critical for remedying the increased occurrence of nitrate-dominated haze event in the NCP.

Data availability. The datasets can be accessed upon request to the corresponding author.

Author contributions. LJ performed the research, designed the analysis approach and wrote the paper. LJ, LZ and HL had the original idea. LZ and HL provided writing guidance and revised the paper. LJ and CL calibrated the HR-ToF-AMS and performed data evaluation. CL provided the ME-2 analysis guidance and the HR-ToF-AMS instrument. LJ and GW operated and maintained the HR-ToF-AMS. All co-authors proofread and commented the manuscript.

https://doi.org/10.5194/acp-2020-213
Preprint. Discussion started: 18 May 2020

Atmospheric Chemistry and Physics Discussions

Competing interests. The authors declare that they have no conflict of interests.

Acknowledgements. This study was supported by the Ministry of Science and Technology of China (Grant nos. 2017YFC0210000), the National Natural Science Foundation of China (Grant Nos. 41705110), Beijing Municipal Natural Science Foundation (8192045) and Beijing Major Science and Technology Project (Z181100005418014). The authors are grateful for the support of the staff of the Xinglong station.

References

Aiken, A., Salcedo, D., Cubison, M. J., Huffman, J., DeCarlo, P., Ulbrich, I. M., Docherty, K. S., Sueper, D., Kimmel, J., and Worsnop, D. R.: Mexico City aerosol analysis during MILAGRO using high resolution aerosol mass spectrometry at the urban supersite (T0)–Part 1: Fine particle composition and organic source apportionment, Atmospheric Chemistry and Physics, 9, 6633-6653, 2009.

Canagaratna, M. R., Jimenez, J. L., Kroll, J. H., Chen, Q., Kessler, S. H., Massoli, P., Hildebrandt Ruiz, L., Fortner, E., Williams, L. R., Wilson, K. R., Surratt, J. D., Donahue, N. M., Jayne, J. T., and Worsnop, D. R.: Elemental ratio measurements of organic compounds using aerosol mass spectrometry: characterization, improved calibration, and implications, Atmospheric Chemistry and Physics, 15, 253-272, 10.5194/acp-15-253-2015, 2015.

Canonaco, F., Crippa, M., Slowik, J. G., Baltensperger, U., and Prévôt, A. S. H.: SoFi, an IGOR-based interface for the efficient use of the generalized multilinear engine (ME-2) for the source apportionment: ME-2 application to aerosol mass spectrometer data, Atmos. Meas. Tech., 6, 3649-3661, 10.5194/amt-6-3649-2013, 2013.

Du, W., Sun, Y., Xu, Y., Jiang, Q., Wang, Q., Yang, W., Wang, F., Bai, Z., Zhao, X., and Yang, Y.: Chemical characterization of submicron aerosol and particle growth events at a national background site (3295 m asl) on the Tibetan Plateau, Atmospheric Chemistry and Physics, 15, 10811-10824, 2015.

Ge, X., Setyan, A., Sun, Y., and Zhang, Q.: Primary and secondary organic aerosols in Fresno, California during wintertime: Results from high resolution aerosol mass spectrometry, Journal of Geophysical Research: Atmospheres, 117, 2012.

Hu, W., Hu, M., Hu, W., Jimenez, J. L., Yuan, B., Chen, W., Wang, M., Wu, Y., Chen, C., Wang, Z., Peng, J., Zeng, L., and Shao, M.: Chemical composition, sources, and aging process of submicron aerosols in Beijing: Contrast between summer and winter, Journal of Geophysical Research: Atmospheres, 121, 1955-1977, 10.1002/2015jd024020, 2016.

Hu, W., Hu, M., Hu, W.-W., Zheng, J., Chen, C., Wu, Y., and Guo, S.: Seasonal variations in high time-resolved chemical compositions, sources, and evolution of atmospheric submicron aerosols in the megacity Beijing, Atmospheric Chemistry and Physics, 17, 9979-10000, 10.5194/acp-17-9979-2017, 2017.

Hu, X.-M., Ma, Z., Lin, W., Zhang, H., Hu, J., Wang, Y., Xu, X., Fuentes, J. D., and Xue, M.: Impact of the Loess Plateau on the atmospheric boundary layer structure and air quality in the North China Plain: A case study, Science of The Total Environment, 499, 228-237, https://doi.org/10.1016/j.scitotenv.2014.08.053, 2014.

Huang, R.-J., Wang, Y., Cao, J., Lin, C., Duan, J., Chen, Q., Li, Y., Gu, Y., Yan, J., Xu, W., Fröhlich, R., Canonaco, F., Bozzetti, C., Ovadnevaite, J., Ceburnis, D., Canagaratna, M. R., Jayne, J., Worsnop, D. R., El-Haddad, I., Prévôt, A. S. H., amp, apos, and Dowd, C. D.: Primary emissions versus secondary formation of fine particulate matter in the top polluted city, Shijiazhuang, in North China, Atmospheric Chemistry and Physics Discussions, 1-38, 10.5194/acp-2018-760, 2018.

Huang, X.-F., He, L.-Y., Hu, M., Canagaratna, M., Kroll, J., Ng, N., Zhang, Y.-H., Lin, Y., Xue, L., and Sun, T.-L.: Characterization of submicron aerosols at a rural site in Pearl River Delta of China using an Aerodyne High-Resolution Aerosol Mass Spectrometer, Atmospheric Chemistry and Physics, 11, 1865-1877, 2011.

Huang, X.-F., Xue, L., Tian, X.-D., Shao, W.-W., Sun, T.-L., Gong, Z.-H., Ju, W.-W., Jiang, B., Hu, M., and He, L.-Y.:

Highly time-resolved carbonaceous aerosol characterization in Yangtze River Delta of China: Composition, mixing state and secondary formation, Atmospheric environment, 64, 200-207, 2013.

Huang, X., Liu, Z., Liu, J., Hu, B., Wen, T., Tang, G., Zhang, J., Wu, F., Ji, D., and Wang, L.: Chemical characterization and source identification of PM 2.5 at multiple sites in the Beijing–Tianjin–Hebei region, China, Atmospheric Chemistry and Physics, 17, 12941, 2017.

Jimenez, J. L.: Ambient aerosol sampling using the Aerodyne Aerosol Mass Spectrometer, Journal of Geophysical Research, 108, 10.1029/2001jd001213, 2003.

Li, H., Zhang, Q., Zhang, Q., Chen, C., Wang, L., Wei, Z., Zhou, S., Parworth, C., Zheng, B., Canonaco, F., Prévôt, A. S. H., Chen, P., Zhang, H., and He, K.: Wintertime aerosol chemistry and haze evolution in an extremely polluted city of North China Plain: significant contribution from coal and biomass combustions, Atmospheric Chemistry and Physics Discussions, 1-31, 10.5194/acp-2016-1058, 2017.

Li, H., Zhang, Q., Zheng, B., Chen, C., Wu, N., Guo, H., Zhang, Y., Zheng, Y., Li, X., and He, K.: Nitrate-driven urban haze pollution during summertime over the North China Plain, Atmospheric Chemistry and Physics, 18, 5293-5306, 10.5194/acp-18-5293-2018, 2018.

Li, H., Cheng, J., Zhang, Q., Zheng, B., Zhang, Y., Zheng, G., and He, K.: Rapid transition in winter aerosol composition in Beijing from 2014 to 2017: response to clean air actions, Atmos. Chem. Phys. Discuss., 2019, 1-26, 10.5194/acp-2019-450, 2019a.

Li, J., Liu, Z., Cao, L., Gao, W., Yan, Y., Mao, J., Zhang, X., He, L., Xin, J., Tang, G., Ji, D., Hu, B., Wang, L., Wang, Y., Dai, L., Zhao, D., Du, W., and Wang, Y.: Highly time-resolved chemical characterization and implications of regional transport for submicron aerosols in the North China Plain, Science of The Total Environment, 135803, https://doi.org/10.1016/j.scitotenv.2019.135803, 2019b.

Li, J., Liu, Z., Gao, W., Tang, G., Hu, B., Ma, Z., and Wang, Y.: Insight into the formation and evolution of secondary organic aerosol in the megacity of Beijing, China, Atmospheric Environment, 220, 117070, https://doi.org/10.1016/j.atmosenv.2019.117070, 2020.

Li, Y., Lee, B., Su, L., Fung, J., and Chan, C.: Seasonal characteristics of fine particulate matter (PM) based on high-resolution time-of-flight aerosol mass spectrometric (HR-ToF-AMS) measurements at the HKUST Supersite in Hong Kong, Atmospheric Chemistry and Physics, 15, 37-53, 2015.

Li, Y. J., Lee, B. Y. L., Yu, J. Z., Ng, N. L., and Chan, C. K.: Evaluating the degree of oxygenation of organic aerosol during foggy and hazy days in Hong Kong using high-resolution time-of-flight aerosol mass spectrometry (HR-ToF-AMS), Atmospheric Chemistry and Physics, 13, 8739-8753, 10.5194/acp-13-8739-2013, 2013.

Liu, Z., Hu, B., Zhang, J., Yu, Y., and Wang, Y.: Characteristics of aerosol size distributions and chemical compositions during wintertime pollution episodes in Beijing, Atmospheric Research, 168, 1-12, 10.1016/j.atmosres.2015.08.013, 2016.

Liu, Z., Gao, W., Yu, Y., Hu, B., Xin, J., Sun, Y., Wang, L., Wang, G., Bi, X., and Zhang, G.: Characteristics of PM 2.5 mass concentrations and chemical species in urban and background areas of China: emerging results from the CARE-China network, Atmospheric Chemistry and Physics, 18, 8849-8871, 2018.

Middlebrook, A. M., Bahreini, R., Jimenez, J. L., and Canagaratna, M. R.: Evaluation of Composition-Dependent Collection Efficiencies for the Aerodyne Aerosol Mass Spectrometer using Field Data, Aerosol Science and Technology, 46, 258-271, 10.1080/02786826.2011.620041, 2012.

Ng, N., Canagaratna, M., Zhang, Q., Jimenez, J., Tian, J., Ulbrich, I., Kroll, J., Docherty, K., Chhabra, P., and Bahreini, R.: Organic aerosol components observed in Northern Hemispheric datasets from Aerosol Mass Spectrometry, Atmospheric Chemistry and Physics, 10, 4625-4641, 2010.

Pan, Y., Wang, Y., Sun, Y., Tian, S., and Cheng, M.: Size-resolved aerosol trace elements at a rural mountainous site in Northern China: importance of regional transport, Science of the Total Environment, 461, 761-771, 2013.

Poulain, L., Spindler, G., Birmili, W., Plass-Dülmer, C., Wiedensohler, A., and Herrmann, H.: Seasonal and diurnal variations of particulate nitrate and organic matter at the IfT research station Melpitz, Atmospheric Chemistry and Physics, 11, 12579-12599, 2011.

https://doi.org/10.5194/acp-2020-213
Preprint. Discussion started: 18 May 2020

Qin, Y. M., Li, Y. J., Wang, H., Lee, B. P. Y. L., Huang, D. D., and Chan, C. K.: Particulate matter (PM) episodes at a suburban site in Hong Kong: evolution of PM characteristics and role of photochemistry in secondary aerosol formation, Atmospheric Chemistry and Physics, 16, 14131-14145, 10.5194/acp-16-14131-2016, 2016.

Seinfeld, J. H., and Pandis, S. N.: Atmospheric chemistry and physics: from air pollution to climate change, John Wiley & Sons, 2016.

Sun, Y., Wang, Z., Fu, P., Jiang, Q., Yang, T., Li, J., and Ge, X.: The impact of relative humidity on aerosol composition and evolution processes during wintertime in Beijing, China, Atmospheric Environment, 77, 927-934, 2013a.

Sun, Y., Du, W., Fu, P., Wang, Q., Li, J., Ge, X., Zhang, Q., Zhu, C., Ren, L., and Xu, W.: Primary and secondary aerosols in Beijing in winter: sources, variations and processes, Atmospheric Chemistry and Physics, 16, 8309-8329, 2016.

Sun, Y., Xu, W., Zhang, Q., Jiang, Q., Canonaco, F., Prévôt, A. S., Fu, P., Li, J., Jayne, J., and Worsnop, D. R.: Source apportionment of organic aerosol from 2-year highly time-resolved measurements by an aerosol chemical speciation monitor in Beijing, China, Atmospheric Chemistry and Physics, 18, 8469-8489, 2018.

Sun, Y. L., Wang, Z. F., Fu, P. Q., Yang, T., Jiang, Q., Dong, H. B., Li, J., and Jia, J. J.: Aerosol composition, sources and processes during wintertime in Beijing, China, Atmospheric Chemistry and Physics, 13, 4577-4592, 10.5194/acp-13-4577-2013, 2013b.

Tao, M., Chen, L., Su, L., and Tao, J.: Satellite observation of regional haze pollution over the North China Plain, Journal of Geophysical Research: Atmospheres, 117, 2012.

Tian, S., Pan, Y., and Wang, Y.: Ion balance and acidity of size-segregated particles during haze episodes in urban Beijing, Atmospheric Research, 201, 159-167, 2018.

Ulbrich, I., Canagaratna, M., Zhang, Q., Worsnop, D., and Jimenez, J.: Interpretation of organic components from Positive Matrix Factorization of aerosol mass spectrometric data, Atmospheric Chemistry and Physics, 9, 2891-2918, 2009.

Wang, Q., Zhao, J., Du, W., Ana, G., Wang, Z., Sun, L., Wang, Y., Zhang, F., Li, Z., and Ye, X.: Characterization of submicron aerosols at a suburban site in central China, Atmospheric environment, 131, 115-123, 2016.

Wang, X., Wei, W., Cheng, S., Yao, S., Zhang, H., and Zhang, C.: Characteristics of PM2. 5 and SNA components and meteorological factors impact on air pollution through 2013–2017 in Beijing, China, Atmospheric Pollution Research, 10, 1976-1984, 2019.

Xu, J., Zhang, Q., Chen, M., Ge, X., Ren, J., and Qin, D.: Chemical composition, sources, and processes of urban aerosols during summertime in northwest China: insights from high-resolution aerosol mass spectrometry, Atmospheric Chemistry and Physics, 14, 12593-12611, 2014.

Xu, J., Zhang, Q., Shi, J., Ge, X., Xie, C., Wang, J., Kang, S., Zhang, R., and Wang, Y.: Chemical characteristics of submicron particles at the central Tibetan Plateau: insights from aerosol mass spectrometry, Atmospheric Chemistry and Physics, 18, 2018.

Xu, W., Han, T., Du, W., Wang, Q., Chen, C., Zhao, J., Zhang, Y., Li, J., Fu, P., Wang, Z., Worsnop, D. R., and Sun, Y.: Effects of Aqueous-Phase and Photochemical Processing on Secondary Organic Aerosol Formation and Evolution in Beijing, China, Environ Sci Technol, 51, 762-770, 10.1021/acs.est.6b04498, 2017.

Yuan, Q., Li, W., Zhou, S., Yang, L., Chi, J., Sui, X., and Wang, W.: Integrated evaluation of aerosols during haze-fog episodes at one regional background site in North China Plain, Atmospheric Research, 156, 102-110, 10.1016/j.atmosres.2015.01.002, 2015.

Zhang, J., Sun, Y., Liu, Z., Ji, D., Hu, B., Liu, Q., and Wang, Y.: Characterization of submicron aerosols during a month of serious pollution in Beijing, 2013, Atmospheric Chemistry and Physics, 14, 2887-2903, 2014a.

Zhang, J., Wang, Y., Huang, X., Liu, Z., Ji, D., and Sun, Y.: Characterization of organic aerosols in Beijing using an aerodyne high-resolution aerosol mass spectrometer, Advances in Atmospheric Sciences, 32, 877-888, 2015.

Zhang, Q., Jimenez, J. L., Worsnop, D. R., and Canagaratna, M.: A case study of urban particle acidity and its influence on secondary organic aerosol, Environmental science & technology, 41, 3213-3219, 2007.

Zhang, Q., Jimenez, J. L., Canagaratna, M. R., Ulbrich, I. M., Ng, N. L., Worsnop, D. R., and Sun, Y.: Understanding atmospheric organic aerosols via factor analysis of aerosol mass spectrometry: a review, Anal Bioanal Chem, 401,

https://doi.org/10.5194/acp-2020-213
Preprint. Discussion started: 18 May 2020

3045-3067, 10.1007/s00216-011-5355-y, 2011.

Zhang, Q., Zheng, Y., Tong, D., Shao, M., Wang, S., Zhang, Y., Xu, X., Wang, J., He, H., and Liu, W.: Drivers of improved PM2. 5 air quality in China from 2013 to 2017, Proceedings of the National Academy of Sciences, 116, 24463-24469, 2019a.

Zhang, X., Xu, J., Kang, S., Zhang, Q., and Sun, J.: Chemical characterization and sources of submicron aerosols in the northeastern Qinghai–Tibet Plateau: insights from high-resolution mass spectrometry, Atmospheric Chemistry and Physics, 19, 7897-7911, 2019b.

Zhang, Y.: Characterization of sub-micron aerosol and its change processes in BIV (Beijing and its vicinity) region, PhD, Meteorology, Chinese Academy of Meteorological Sciences, China Meteorological Administration, Beijing, 2011.

Zhang, Y., Zhang, X., Sun, J., Hu, G., Shen, X., Wang, Y., Wang, T., Wang, D., and Zhao, Y.: Chemical composition and mass size distribution of PM 1 at an elevated site in central east China, Atmospheric Chemistry and Physics, 14, 12237-12249, 2014b.

Zhao, D., Xin, J., Gong, C., Quan, J., Liu, G., Zhao, W., Wang, Y., Liu, Z., and Song, T.: The formation mechanism of air pollution episodes in Beijing city: Insights into the measured feedback between aerosol radiative forcing and the atmospheric boundary layer stability, Science of The Total Environment, 692, 371-381, 2019.

Zhu, Q., He, L.-Y., Huang, X.-F., Cao, L.-M., Gong, Z.-H., Wang, C., Zhuang, X., and Hu, M.: Atmospheric aerosol compositions and sources at two national background sites in northern and southern China, Atmospheric Chemistry and Physics, 16, 10283-10297, 2016.